JOURNAL OF MATERIALS SCIENCE 13 (1978) 1006–1014

Ln-M-O glasses obtained by rapid quenching using a laser beam

TOETSU SHISHIDO, KIYOHITO OKAMURA, SEISHI YAJIMA
Oarai Branch, Research Institute for Iron, Steel and Other Metals, Tohoku University, Ibaraki-ken, 311-13, Japan

A rapid quenching apparatus employing a laser beam was developed to obtain the glassy state of oxides which have high melting temperatures. Using this apparatus, the glassy state in Ln–Ti–O, Ln–Nb–O and Ln–Ta–O (Ln = lanthanides) systems was investigated. The range of compositions which produced glasses and the crystallization process were studied in detail, and the metastable phases, which appear during the crystallization process, were examined by differential thermal and X-ray diffraction analysis.

1. Introduction

It is known that oxides can be obtained in the glassy state by rapid quenching. Sarjeant and Roy [1] produced the glassy states of V_2O_5, MoO_3, WO_3 and TeO_2 by splat-cooling techniques. The glassy state of $BaO–Fe_2O_3$ was obtained by Kantor *et al.* [2], while that of $La_2O_3–WO_3$ was obtained by Yoshimura *et al.* [3]. Suzuki and Anthony studied the possibility of producing non-crystalline solids of many oxide compounds by rapid quenching [4].

The present authors have studied the vitrification of high melting point oxides having a lanthanide oxide (Ln_2O_3) as the main component. As these oxides are comparatively difficult to turn into the glassy state, three special rapid quenching apparatuses have been developed [5, 6], and with their help the glassy states in the Ln–Al–O [5, 7], Ln–Ga–O [8] and Ln–Fe–O [9] systems could be realized. In these glasses the metallic elements have the same trivalent state as the Ln elements. The objective of the present study was to obtain the glassy state of the $Ln–Ti^{4+}–O$, $Ln–Nb^{5+}–O$ and $Ln–Ta^{5+}–O$ systems where the metal ions have a higher valency. Furthermore, the crystallization process of these glasses was examined in relation to the various Ln elements.

2. Experimental

2.1. Materials

As starting materials, 99.9% pure powder of Ln_2O_3*, TiO_2, Nb_2O_5 and Ta_2O_5 were used. The size of the powder was under 325 mesh. The various oxide powders were mixed to obtain initial batches of different molar ratios. These powders were cold pressed at 4000 kg cm^{-2} into pellets of 5 mm diameter and 1 mm thickness. Sintering of the pellets was carried out at 1000° C for 5 h in air. Subsequently the sintered pellets were crushed into small pieces of 1 to 2 mm in diameter, which were placed into the melting apparatus as shown in Fig. 1. Melting was carried out by means of a laser beam, which was directed to the sample through a germanium lens. The melt could be quenched rapidly by using the piston and anvil technique.

2.2. Rapid quenching apparatus

Rapid quenching was achieved by using the conventional piston, hammer and anvil method inside the laser melting furnace (Fig. 1). The small samples were placed into the flat depression of the water-cooled copper disc of the furnace, which also served as the cold anvil. Ten samples could be placed on the copper disc, which was then

*CeO_2, Pr_6O_{11} and Tb_4O_7 were used in the case of Ln = Ce, Pr, and Tb, respectively.

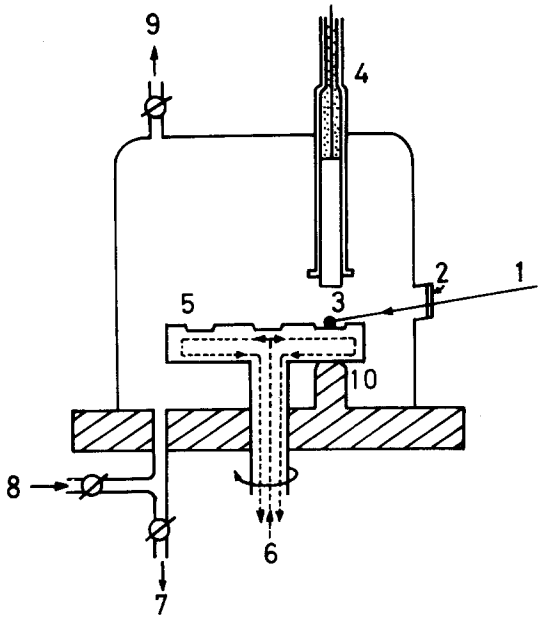

Figure 1 Rapid quenching apparatus incorporating a laser beam; (1) laser beam, (2) germanium lens, (3) sample to be quenched, (4) pneumatic hammer, (5) copper disc (anvil), (6) cooling water, (7) to vacuum pump, (8) inert gas inlet. (9) inert gas outlet, (10) anvil support.

rotated to bring each sample into the correct position between the hammer and the anvil support. The piston was driven by compressed air at a pressure of up to 100 kg cm^{-2}. Neglecting friction, the terminal velocity is given by $V = (2PX_0/m)^{1/2}$ (P = air pressure, X_0 = distance between piston and anvil, m = mass of piston). From this equation the maximum terminal velocity was calculated to be 100 m sec^{-1}. For smaller velocities the piston could be activated either by a spring or manually. The laser beam equipment was a continuous wave (CW) CO_2 laser (10.6 μm) from the Japan Electron Optics Laboratory, operating with a gas mixture of molar ratio $CO_2 : N_2 : He = 1:2:7$ and a maximum power output of 250 W. The laser beam was focused onto the sample by a germanium lens situated in the wall of the melting apparatus. The temperature of the molten sample was measured with an optical pyrometer.

2.3. Observation and analysis

2.3.1. Polarizing microscope observation

A polarizing transmission microscope (Olympus Model POM) was used to determine whether the specimens were in the glassy or crystalline state. The specimens were placed between the crossed Nicols and the variation of the contrast in the microscope image due to the rotation of the specimen was observed.

2.3.2. Differential thermal analysis

The thermal properties of the glassy samples were measured by differential thermal analysis (DTA). The apparatus used was a Model TG-DTA high temperature microbalance from the Rigaku Denki Co. Ltd. The glassy samples were prepared as thin films and placed into a platinum cell. As a standard, a sample of high purity α-Al_2O_3 powder was used. DTA was performed during raising and lowering of the temperature at a rate of 10° C min^{-1} in a flowing argon gas atmosphere. Calibration of the measured temperatures was made with the transition temperatures of $BaCO_3$, $SrCO_3$ and Na_2MnO_4, or with the melting temperature of Na_2SO_4. The error in the temperature measurement was within ± 2° C. The values for the heat of crystallization of the test specimens were corrected with respect to the known transition heats or melting heats of standard reagents.

2.3.3. X-ray diffraction analysis

The X-ray powder diffraction method was used to characterize the rapidly quenched samples and to determine the phases which appeared during the crystallization process. The diffraction patterns were obtained with Ni-filtered CuKα radiation

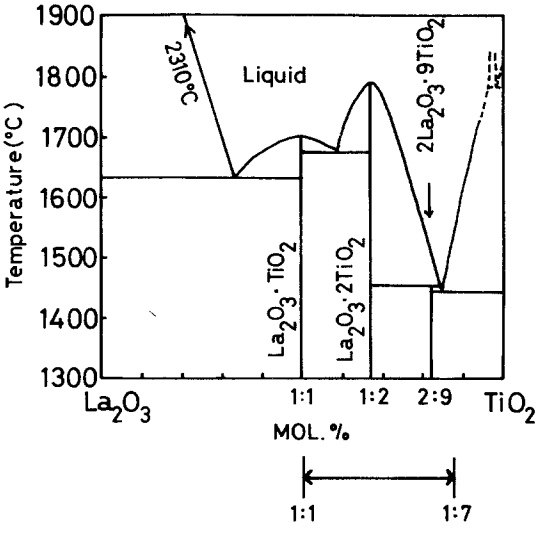

Figure 2 Phase diagram of La_2O_3–TiO_2, and the composition range giving a glassy state (↔).

and using a Debye–Scherrer camera of 114.6 mm radius. The measured diffraction angles were corrected by using a standard sample of 99.999% purity silicon powder. The crystal structures of the unknown phases were determined as follows: first, indexes were assigned to the principal lines with the help of Hull–Davy's charts. Subsequently, the remaining lines were indexed by determining the integral values of h, k and l which fitted the respective $\sin^2\theta$ values obtained from the diffraction pattern [10]. The lattice constants were then determined by means of the Nelson–Riley's function. The relative intensities of the difffaction lines were measured with a diffractometer equipped with a scintillation counter and a pulse-height analyser.

3. Results and discussion

3.1. The cooling rate of the quenching apparatus

The cooling rate of the rapid quenching apparatus shown in Fig. 1 was calculated from the formula [11]:

$$T = \Delta T/\Delta t \approx (T_t - T_g)/\Delta t$$

where T_t = temperature of the molten sample (° C)

T_g = glass transition temperature (° C)

Δt = duration of contact between the sample and the piston of the quenching apparatus (sec).

The cooling rate was determined by using a standard sample of $Nd_2O_3 \cdot 5Nb_2O_5$ of thickness of 1 mm. This material has a glass transition temperature $T_g = 680°$ C. After melting and heating the sample to $T_t = 1500°$ C, it could be vitrified by quenching it at a piston speed of 100 m sec^{-1}. The duration of quenching, Δt, was obtained as about 10^{-5} sec by dividing the sample thickness by the piston speed. These values inserted into the above formula give a cooling rate of

$$T \approx 8.2 \times 10^7 \ (° \text{C sec}^{-1})$$

3.2. Glasses in the $Ln_2O_3-TiO_2$ system

Various sintered bodies of the composition $Ln_2O_3 \cdot xTiO_2$ were prepared by using various Ln elements and molar oxide ratios, x. These sintered test pieces were then melted and rapidly quenched as described above. The products obtained were brown in colour and could be classified into three groups when viewed in visible light, namely as transparent, semi-transparent, and opaque. The glassy state of the transparent samples was confirmed by observation in the polarizing microscope and by X-ray powder analysis. The crystalline phases of the semi-transparent and opaque samples were investigated by the X-ray powder method. In this way the kinds of Ln elements and the composition range which gave a glassy state could be determined.

In the $Ln_2O_3 \cdot xTiO_2$ system, glasses were obtained for Ln = La, Ce, Pr, Nd, Sm, Eu, Gd, and Tb and within the composition range of $1 < x < 7$. For the other Ln elements a complete glassy state could not be realized for any value of x. For example in the case of $2Ho_2O_3 \cdot 9TiO_2$, the quenched product was semi-transparent and observation in the polarizing microscope showed that it was a mixture of glassy and crystalline phases. X-ray analysis indicated the crystalline phases to be $Ho_2O_3 \cdot 2TiO_2$ and TiO_2.

Fig. 2 shows the phase diagram [12] of the $Ln_2O_3-TiO_2$ system for Ln = La, and the composition range in which a glassy state was obtained. As indicated in the phase diagram, the eutectic with the lowest melting point exists in the vicinity of $2La_2O_3 \cdot 9TiO_2$ [12, 13]. Near this composition the $La_2O_3-TiO_2$ oxides could be converted into the glassy state relatively easily, i.e. at a lower cooling speed than for other compositions. This result is in agreement with the general observation that a eutectic melt having a high viscosity has a strong tendency to vitrify during rapid quenching [14]. Assuming that the glass-forming oxides of the remaining Ln elements show similar behaviour to the above $La_2O_3-TiO_2$ oxides, further studies were confined to the composition $2Ln_2O_3 \cdot 9TiO_2$. Eight types of glasses were prepared and the influence of the various Ln elements on the crystallization process during heating at a constant rate was measured by DTA and X-ray powder analysis.

The results of the DTA measurements are given in Fig. 3. In raising the temperature, one exothermic peak appeared for Ln = Ce, Sm, Eu, Gd and Tb, while two such peaks appeared for Ln = La, Pr and Nd. In the case of Ln = Ce and Sm the peaks do not have a symmetrical shape. Furthermore, it was observed that for all samples the base line bends slightly in the endothermic direction at a particular temperature, which is about 30° C lower than that of the beginning of the first peak. This temperature corresponds

TABLE I Thermal properties of $2Ln_2O_3 \cdot 9TiO_2$ glasses.

Ln in $2Ln_2O_3 \cdot 9TiO_2$ glass	Glass transition temperature T_g (° C)	Crystallization temperature $T_{c_{max}}$	Crystallization heat ΔH_c^* (kcal mol^{-1})
La	772	807	0.39
		837	0.65
Ce	760	792	1.31
Pr	810	849	1.10
		900	0.10
Nd	765	807	1.38
		900	0.24
Sm	765	816	1.29
Eu	755	795	0.59
Gd	765	804	1.08
Tb	765	795	1.11

*These heat values are calculated for $Ln_{4/37}Ti_{9/37}O_{24/37}$.

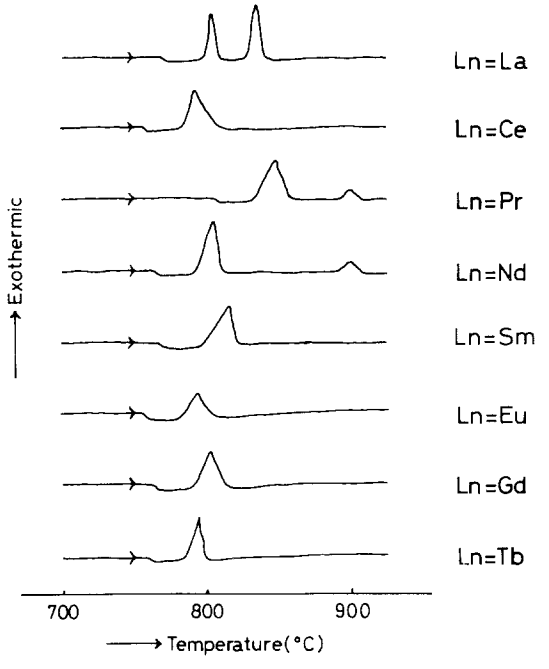

Figure 3 DTA curves of $2Ln_2O_3 \cdot 9TiO_2$ glasses.

to the glass transition point (T_g). While lowering the temperature, no exothermic or endothermic peaks were observed. The thermal analysis was repeated three times for each sample and the scatter in the exothermic peaks and in the peak areas were only ± 2° C and ± 0.03 kcal mol^{-1} respectively.

From the areas of the exothermic peaks the heat of crystallization can be calculated, and the respective values are shown in Table I for Ln = La to Tb. Although some specimens have two exothermic peaks, the heats of crystallization obtained from the first peak are all in the vicinity of 1 kcal mol^{-1}, except for Ln = La and Eu.

In order to obtain detailed information on the crystallization process, the specimens were removed from the DTA apparatus at the temperatures of the exothermic peaks, and were subsequently subjected to X-ray powder analysis. The results obtained were different according to the type of Ln element.

3.2.1. Crystallization process of $2Ln_2O_3 \cdot 9TiO_2$ glasses with Ln = La, Pr and Nd

At temperatures just below the first exothermic peak, X-ray diffraction of each specimen gave the halo patterns typical of the glassy state. When the specimens were heated to a temperature just above the first exothermic peak, new single crystalline phases were found. These phases were different from those observed in samples which crystallized during quenching from the melt. Structure analysis showed that the new phases belonged to the hexagonal system, and the lattice constant obtained for each Ln element are given in Table II. To demonstrate the good correlation between the measured diffraction lines and the crystal structure assigned to the new phases, Table III compares the observed and calculated lattice

TABLE II Crystallographic properties of the metastable phase formed on heating $2Ln_2O_3 \cdot 9TiO_2$ glasses.

Glass system	Metastable phase	Lattice constants		
		a(Å)	c(Å)	c/a
La–Ti–O	hexagonal	9.410	6.477	0.688
Pr–Ti–O	hexagonal	9.335	6.444	0.690
Nd–Ti–O	hexagonal	9.329	6.431	0.689

TABLE III Values of d_{obs} and d_{calc} of the metastable phase formed on heating $2La_2O_3 \cdot 9TiO_2$ glass.

hkl	d_{obs}(Å)	d_{calc}(Å)	I_{obs}
201	3.449	3.449	VS
002	3.233	3.238	VS
202	2.538	2.535	M
310	2.254	2.260	VVW
221	2.198	2.211	VVW
320	1.870	1.870	VW
402	1.724	1.724	VW
004	1.619	1.619	VW
501	1.583	1.581	VVW
420	1.540	1.540	VW

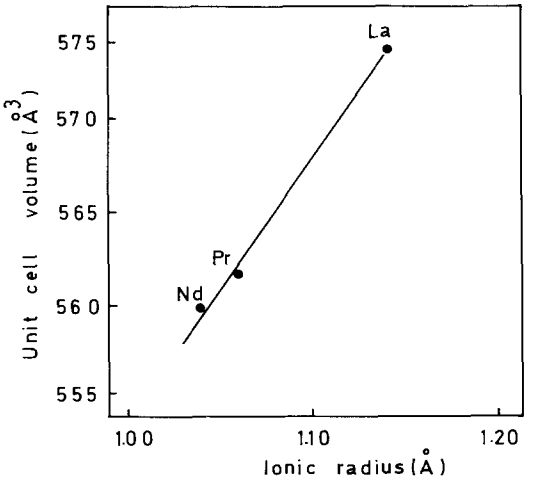

Figure 4 Relationship between the radius of Ln^{3+} ions (six-coordination) and the unit cell volume of metastable phases which form on heating $2Ln_2O_3 \cdot 9TiO_2$ glasses.

spacings for Ln = La. Fig. 4 shows the relationship between the radius for the Ln (III) ion (six-coordination), and the unit cell volume of the new phase compound. It is seen that the size of the lanthanide strongly influences the unit cell volume.

When the samples were heated to a temperature just above the second peak the well-known stable phase $2Ln_2O_3 \cdot 9TiO_2$ appeared and was the only phase found. From these results it was established that the crystallization process of $2Ln_2O_3 \cdot 9TiO_2$ glasses with Ln = La, Pr, and Nd occurs in two stages. At the temperature of the first exothermic peak a new metastable phase is formed. This metastable phase then converts into the stable phase at a higher temperature, which corresponds to the second exothermic peak.

3.2.2. Crystallization process in $2Ln_2O_3 \cdot 9TiO_2$ glasses with Ln = Ce, Sm, Eu, Gd and Tb.

For these glasses, only one exothermic peak was found in the DTA curves. Samples heated to a temperature just above this peak gave X-ray patterns which corresponded to the stable phases. Thus in these oxide systems, the stable phase forms directly from the glassy state, without an intermediate metastable phase.

3.3. Glasses in the $Ln_2O_3-Nb_2O_5$ systems

In the $Ln_2O_3 \cdot xNb_2O_5$ systems with Ln = La, Ce, Pr, Nd, Sm, Eu and Gd the glassy state again was

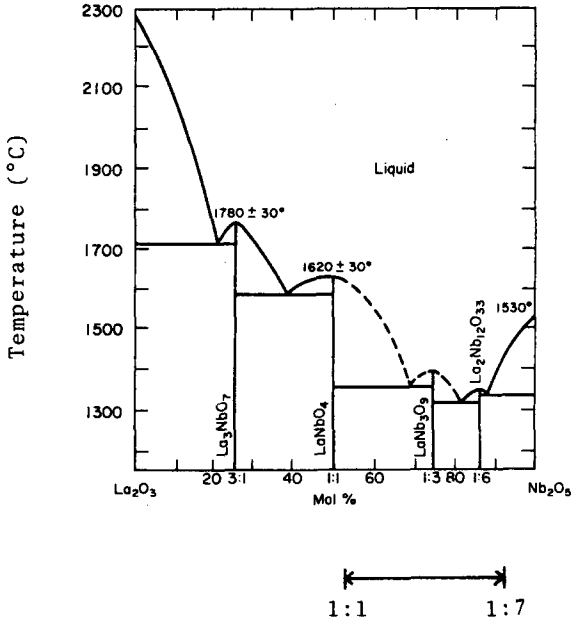

Figure 5 Phase diagram of $La_2O_3-Nb_2O_5$, and the composition range giving a glassy state (↔).

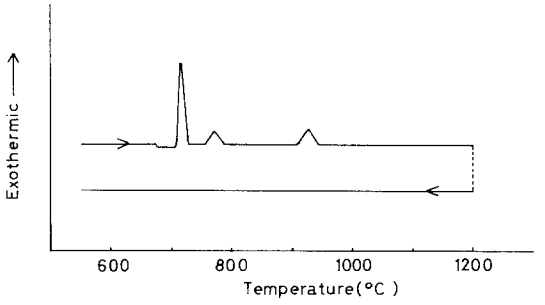

Figure 6 DTA curve of $La_2O_3 \cdot 5Nb_2O_5$ glass.

obtained in the composition range of $1 < x < 7$. The glasses had a brown colour and were transparent to visible light. With the other Ln elements however, such as for example Ho, which is a heavy rare earth element, a single glassy phase could not be realized for any value of x.

Fig. 5 shows the phase diagram of the $La_2O_3 - Nb_2O_5$ system [15] together with the composition range in which vitrification could be achieved. As indicated in the phase diagram, eutectics exist in the composition range $x = 3$ to 7. For the same reasoning as for the previously discussed $Ln_2O_3 \cdot xTiO_2$ samples, further investigation was confined to $Ln_2O_3 \cdot 5Nb_2O_5$ in the vicinity of eutectic composition and seven different glasses were prepared with the Ln element varying from La to Gd. The crystallization process on heating at a constant rate was again investigated by DTA and X-ray powder analysis.

Fig. 6 shows the DTA curve for Ln = La and it is seen that three exothermic peaks appear on heating. The base line bends slightly towards the endothermic side at a temperature which is 30° C lower than that of the beginning of the first peak, indicating the glass transition temperature (T_g). On cooling, no exothermic or endothermic peaks were observed. The remaining glasses with Ln = Ce to Gd also gave three exothermic peaks similar to those for Ln = La.

The heats of crystallization, calculated from the areas of the exothermic peaks, are given in Table IV. In each case the first peak has the largest area, which corresponds to a crystallization heat of 0.4 to 1 kcal mol^{-1}.

Specimens of the various glasses were removed from the DTA apparatus at temperatures just above each of the exothermic peaks and X-ray analysis was performed. Just below the first peak the samples were still completely in the glassy state, as indicated by the typical halo patterns. Raising the temperature just above the first peak resulted in the formation of a new metastable phase. Such a metastable phase occurred

TABLE IV Thermal properties of $Ln_2O_3 \cdot 5Nb_2O_5$ glasses.

Ln in $Ln_2O_3 \cdot 5Nb_2O_5$ glass	Glass transition temperature T_g (° C)	Crystallization temperature $T_{c_{max}}$ (° C)	Crystallization Heat ΔH_c^* (kcal mol^{-1})
La	687	714	0.97
		771	0.42
		922	0.51
Ce	675	705	0.87
		759	0.34
		942	0.83
Pr	675	705	0.77
		771	0.25
		942	0.60
Nd	684	705	0.38
		777	0.07
		930	0.25
Sm	672	705	0.73
		771	0.45
		924	0.10
Eu	678	699	0.77
		756	0.54
		924	0.35
Gd	684	708	0.45
		744	0.07
		924	0.03

*These heat values are calculated for $Ln_{2/40}Nb_{10/40}O_{28/40}$.

TABLE V Crystallographic properties of the metastable phases formed on heating $Ln_2O_3 \cdot 5Nb_2O_5$ glasses.

Glass system	Metastable phase	Lattice constants		
		a (Å)	c (Å)	c/a
La–Nb–O	hexagonal	7.400	4.240	0.573
Ce–Nb–O	hexagonal	7.928	4.503	0.568
Pr–Nb–O	hexagonal	7.325	4.234	0.578
Nd–Nb–O	hexagonal	7.300	4.207	0.576
Sm–Nb–O	hexagonal	7.288	4.210	0.578
Eu–Nb–O	hexagonal	7.370	4.300	0.583
Gd–Nb–O	hexagonal	7.244	4.245	0.586

TABLE VI Values of d_{obs} and d_{calc} of the metastable phase formed on heating $La_2O_3 \cdot 5Nb_2O_5$ glass.

hkl	d_{obs} (Å)	d_{calc} (Å)	I/I_1
1 1 0	3.705	3.700	60
2 0 0	3.195	3.204	100
1 1 1	2.777	2.788	20
0 0 2	2.120	2.120	20
2 2 0	1.850	1.850	50
4 0 0	1.601	1.602	30
3 2 0	1.470	1.470	20
4 2 0	1.212	1.211	20

for all Ln elements, and structure analysis showed that they belonged to the hexagonal system. The lattice constants of these metastable phases are given in Table V, while Table VI shows the good agreement between the observed lattice spacings and those calculated from the assigned lattice constants for the case of Ln = La. Fig. 7 gives the relationship between the radius of the Ln (III) ion (six-coordination) and the lattice constants of the metastable hexagonal compounds. The influence of the size of the lanthanide on the lattice constant a is especially strong. Furthermore it is seen from Fig. 7 that the lattice constants for the phases with Ln = Ce and Eu do not lie on the straight line connecting the a and c values of the other Ln elements. This deviation from the expected values is due to the conversion of Eu^{3+} to E^{2+} during laser heating, as Eu is relatively easy to reduce. The same is true for Ce, which also converts from the Ce^{3+} state to one of lower valency [16]. X-ray fluorescence analysis confirmed this explanation.

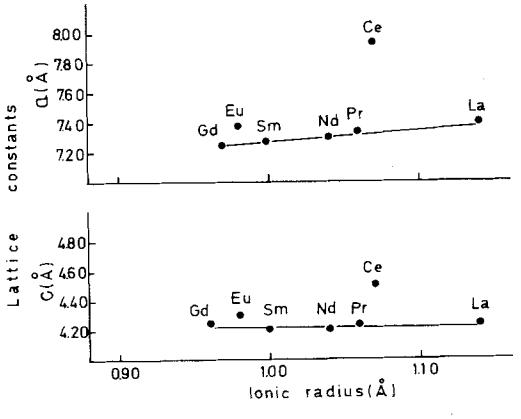

Figure 7 Relationship between the radius of Ln^{3+} ions (six-coordination) and the unit cell volume of metastable phases which form on heating $Ln_2O_3 \cdot 5Nb_2O_5$ glasses.

At the temperature just above the second exothermic peak a mixture of the above metastable phase and the stable phase was observed for all specimens. For instance in the case of Ln = La, the specimens contained a mixture of the metastable hexagonal phase and the stable $La_2O_3 \cdot 5Nb_2O_5$ phase. Crystal data of $La_2O_3 \cdot 6Nb_2O_5$ in the phase diagram were not reported. Identification of the phase after crystallization was obtained from the data of $La_2O_3 \cdot 5Nb_2O_5$ [17, 18]. Finally, at temperatures above the third exothermic peak, only the stable phase was found.

Thus the first, second and third exothermic peaks observed in DTA are due to the crystallization of a new metastable phase, the precipitation of $Ln_2O_3 \cdot 5Nb_2O_5$ and the complete transition to the stable phase $Ln_2O_3 \cdot 5Nb_2O_5$.

3.4. Glasses in the Ln_2O_3–Ta_2O_5 system

In the Ln_2O_3–Ta_2O_5 system, glasses could only be obtained for Ln = La, Ce, Pr, Nd, Sm, Eu and Gd and within the composition range $1 < x < 7$. The glasses had a brown colour and were transparent to visible light. For the other Ln elements, a complete glassy state could not be realized for any composition.

Fig. 8 relates the phase diagram of the La_2O_3–Ta_2O_5 system [19] to the composition range for which glasses were obtained. Selecting $3Ln_2O_3 \cdot 7Ta_2O_5$ in the vicinity of eutectic composition with reference to the phase diagram [20–22], glassy samples were prepared for Ln = La to Gd and the crystallization process was studied as for the preceding oxide systems.

The results of DTA measurements were similar for all Ln elements and, as shown in Fig. 9 for the case of Ln = La, only one exothermic peak was found on heating. The glass transition temperature is indicated by the deviation of the base line towards the endothermic side. No peaks were found during cooling. The heats of crystallization,

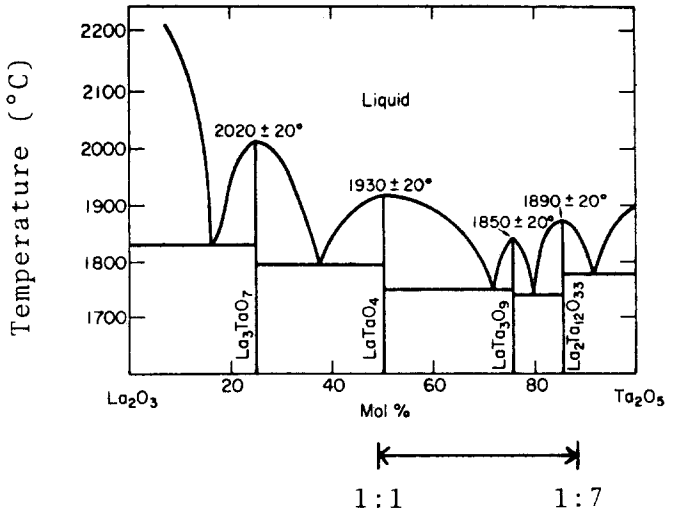

Figure 8 Phase diagram of La_2O_3–Ta_2O_5, and the composition range giving a glassy state (↔).

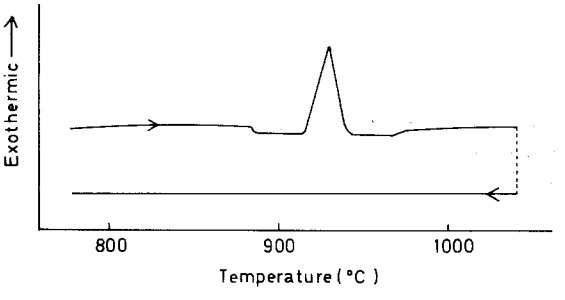

Figure 9 DTA curve of $3La_2O_3 \cdot 7Ta_2O_5$ glass.

as calculated from the areas of the exothermic peaks, are given in Table VII.

X-ray diffraction analysis of samples heated to temperatures just below and above the exothermic peak revealed that below the peak the samples were still completely glassy. At higher temperatures above the exothermic peak the samples contained the stable phases, which for example in the case of Ln = La were mixed phases of $LaTaO_4$ and $LaTa_3O_9$.

Thus it is established that the crystallization process of $3Ln_2O_3 \cdot 7Ta_2O_5$ glasses involves the direct formation of the stable phases, without any intermediate metastable phase.

4. Conclusion

A rapid quenching apparatus using a Co_2 laser beam was developed to obtain glasses in the $Ln_2O_3 \cdot xTiO_2$, $Ln_2O_3 \cdot xNb_2O_5$ and $Ln_2O_3 \cdot xTa_2O_5$ systems. For all systems the formation of glasses was found to depend on two conditions, namely that the Ln elements are light to medium heavy elements and that the composition lies within the range of $1 < x < 7$. The crystallization characteristics of the glasses were studied for samples with compositions of $2Ln_2O_3 \cdot 9TiO_2$, $Ln_2O_3 \cdot 5Nb_2O_5$ and $3Ln_2O_3 \cdot 7Ta_2O_5$ respectively. The results are summarized in Table VIII and it is seen that the crystallization process is influenced by the Ln element and the transition metal.

A metastable phase forms prior to the appearance of the stable phase in the case of $2Ln_2O_3 \cdot 9TiO_2$ glasses with Ln = La, Pr and Nd, and in the case of $Ln_2O_3 \cdot 5Nb_2O_5$ glasses with Ln = La to Gd. These metastable phases have a hex-

TABLE VII Thermal properties of $3Ln_2O_3 \cdot 7Ta_2O_5$ glasses.

Ln in $3Ln_2O_3 \cdot 7Ta_2O_5$ glass	Glass transition temperature T_g (° C)	Crystallization temperature $T_{c_{max}}$ (° C)	Crystallization heat ΔH_c* (kcal mol^{-1})
La	886	930	0.98
Ce	865	910	1.38
Pr	877	921	2.55
Nd	862	906	0.22
Sm	866	910	0.40
Eu	855	900	2.50
Gd	871	916	1.00

*These heat values are calculated for $Ln_{6/64}Ta_{14/64}O_{44/64}$.

TABLE VIII Crystallization process of Ln–M–O glasses (Ln = Lanthanides, M = Ti, Nb, Ta).

$2Ln_2O_3 \cdot 9TiO_2$ (Ln = Ce, Sm, Eu, Gd, Tb) $3Ln_2O_3 \cdot 7Ta_2O_5$ (Ln = La to Gd)	Glassy phase → Stable phase
$2Ln_2O_3 \cdot 9TiO_2$ (Ln = La, Pr, Nd)	Glassy phase → Metastable phase → Stable phase
$Ln_2O_3 \cdot 5Nb_2O_5$ (Ln = La to Gd)	Glassy phase → Metastable phase → {Metastable phase + Stable phase} → Stable phase

agonal crystal structure, and the lattice constants of these phases are influenced by the size of the lanthanides.

References

1. P. T. SARJEANT and R. ROY, *J. Amer. Ceram. Soc.* **50** (1967) 500.
2. P. KANTOR, A. REVCOLEVSCHI and R. COLLONGUES, *J. Mater. Sci.* 8 (1973) 1359.
3. M. YOSHIMURA, J. COUTURES and M. FOEX, *ibid* **12** (1977) 415.
4. T. SUZUKI and A. M. ANTHONY, *Mater. Res. Bull.* 9 (1974) 745.
5. S. YAJIMA, K. OKAMURA and T. SHISHIDO, *Chem. Lett.* (1973) 741.
6. *Idem,* "Proceedings of the 11th Rare Earth Research Conference", Vol. II, edited by M. Haschke and H. A. Eick (United States Atomic Energy Commission Technical Information Center, Oak Ridge, Tennessee, 1974) p. 568.
7. *Idem, Chem. Lett.* (1973) 1327.
8. *Idem, ibid* (1974) 545.
9. *Idem, ibid* (1974) 1531.
10. H. LIPSON and H. STEEPLE, "Interpretation of X-ray Powder Diffraction Patterns" (Macmillan, London, 1968) p. 125.
11. H. S. CHEN and C. E. MILLER, *Rev. Sci. Instrum.* **41** (1970) 1237.
12. J. B. MAC CHENSNEY and H. A. SAUER, *J. Amer. Ceram. Soc.* **45** (1962) 416.
13. T. F. LIMAR, N. G. KISEL, I. F. CHEREDNICHENKO and L. P. MUDROLYUBOVA, *Izv. An. SSSR, Neorg. Mater.* **10** (1974) 1826.
14. H. RAWSON, "Inorganic Glass Forming Systems" (Academic Press, London and New York, 1967).
15. N. A. GODINA, E. P. SABCHENKO and E. K. KELER, *Dokl. Akad. Nauk. SSSR* **178** (1968) 1324.
16. B. G. HYDE and L. EYRING, "Proceedings of the 4th Conference on Rare Earth Research", (Gordon and Breach Science Publishers, New York, London, Paris, 1964) p. 654.
17. V. K. TRUNOV and L. M. KOVBA, *Russ. J. Inorg. Chem.* **11** (1966) 1298.
18. M. DANIEL BODIOT, *C. R. Akad. Sci. Paris* **268** (1969) 163.
19. N. S. AFONSKII and M. NEIMAN, *Izv. An. SSSR, Neorg. Mater.* 3 (1967) 1280.
20. M. M. PINAEVA, E. I. KRYLOV and V.M. RYAKOV, *ibid* 3 (1967) 1612.
21. *Idem., ibid.* 4 (1968) 982.
22. R. S. ROTH, J. L. WARING and W. S. BROWER, *J. Res. Nat. Bur. Stand.* 74 (1970) 482.

Received 5 July and accepted 21 September 1977.